Astron. Astrophys. 319, 52–66 (1997)

ASTRONOMY
AND
ASTROPHYSICS

AGNs with composite spectra⋆

P. Véron[1], **A.C. Gonçalves**[1,2], **and M.-P. Véron-Cetty**[1]

[1] Observatoire de Haute-Provence (CNRS), F-04870 Saint Michel l'Observatoire, France
[2] Centro de Astrofísica da Universidade do Porto, Rua do Campo Alegre 823, 4150 Porto, Portugal

Received 11 April 1996 / Accepted 22 July 1996

Abstract. The use of the Baldwin et al. (1981) or Veilleux & Osterbrock (1987) diagnostic diagrams allows the unambiguous classification of the nuclear emission line regions of most galaxies into one of three categories: nuclear HII regions or starbursts, Seyfert 2 galaxies and Liners. However, a small fraction of them have a "transition" spectrum.

We present spectral observations of 15 "transition" objects at high-dispersion (66Åmm^{-1}) around the Hα, [NII]$\lambda\lambda$6548, 6584 and/or Hβ, [OIII]$\lambda\lambda$4959, 5007 emission lines. We show that most of these spectra are composite, due to the simultaneous presence on the slit of a Seyfert nucleus and a HII region.

Seyfert 2s and Liners seem to occupy relatively small and distinct volumes in the three-dimensional space $\lambda5007/\mathrm{H}\beta$, $\lambda6584/\mathrm{H}\alpha$, $\lambda6300/\mathrm{H}\alpha$.

Key words: galaxies: nuclei – galaxies: active – galaxies: Seyfert

1. Introduction

Baldwin et al. (1981) have shown empirically that several combinations of easily-measured emission lines can be used to separate emission-line galaxies into one of three categories according to the principal excitation mechanism: nuclear HII regions or starbursts, Seyfert 2 galaxies and Liners. They have found that the three groups can be effectively segregated using plots of [NII]$\lambda6584/\mathrm{H}\alpha$ *vs*. [OIII]$\lambda5007/\mathrm{H}\beta$ and of [OII]$\lambda3727/$[OIII]$\lambda5007$ *vs*. [OIII]$\lambda5007/\mathrm{H}\beta$, [NII]$\lambda6584/\mathrm{H}\alpha$, or [OI]$\lambda6300/\mathrm{H}\alpha$.

Veilleux & Osterbrock (1987) have proposed a revised method of classification involving the line ratios $\lambda5007/\mathrm{H}\beta$, $\lambda6584/\mathrm{H}\alpha$, [SII]$\lambda\lambda6717, 6731/\mathrm{H}\alpha$ and $\lambda6300/\mathrm{H}\alpha$. These line ratios take full advantage of the physical distinctions between the various types of objects and minimize the effects of reddening correction and calibration errors.

Send offprint requests to: P. Véron

⋆ Based on observations made at the Observatoire de Haute-Provence (CNRS), France

The use of Baldwin et al. (1981) or Veilleux & Osterbrock (1987) diagnostic diagrams generally yields an immediate classification of the nuclear emission line clouds; "transition" objects exist however, which cannot be classified unambiguously from their line ratios (Heckman et al., 1983; Keel, 1984; Veilleux & Osterbrock, 1987; Ho et al., 1993a). When observed with sufficient spectral resolution, such objects show different profiles for the permitted and forbidden lines (Heckman et al., 1981; Véron et al., 1981a,b; Véron-Cetty & Véron, 1985, 1986b), this being due to the superposition of several components that have different relative line strengths and are kinematically and spatially distinct - usually a HII region and a Seyfert cloud; they have a "composite" spectrum.

The fraction of giant spiral galaxies with Seyfert or Liner like activity decreases from about 70% in Sa to 6% in Sc; in contrast, the fraction of galaxies with a nuclear HII region rises from 4% in Sa to 65% in Sc (Véron-Cetty & Véron, 1986b). If the occurence of the two kinds of emission line regions is independent, we expect to find them simultaneously in 3 to 6% of all nuclei, with a maximum in Sb galaxies; the existence of composite spectra is therefore not unexpected.

The aim of this paper is to check the hypothesis that HII regions, Liners and Seyfert 2s fall into well defined and relatively restricted regions in the $\lambda5007/\mathrm{H}\beta$ *vs*. $\lambda6584/\mathrm{H}\alpha$ and other similar diagrams, and that all "transition" spectra are in fact composite spectra. If this is the case, the regions occupied by Liners and Seyfert 2s in such diagnostic diagrams will have a smaller area, restricting the range of possible physical parameters in these clouds.

2. Nuclear emission regions

2.1. HII regions

A large fraction of all spiral galaxies exhibit a nuclear emission-line spectrum which ressembles a stellar-photoionized HII region (Keel, 1983b; Véron-Cetty & Véron, 1986b). These objects are called HII region nuclei, or, in unusually luminous cases, starburst nuclei (Weedman et al., 1981; Balzano, 1983; Heckman et al., 1983). Some galaxies also contain discrete circumstellar HII regions referred to as hotspots (Sersic & Pastoriza,

1965). The emission-line spectra of these nebulae form a one-parameter (the ionizing parameter) sequence (Evans & Dopita, 1985; McCall et al., 1985).

2.2. Seyfert galaxies

Koski (1978) found that the optical continua of Seyfert 2 nuclei could be approximated by a stellar contribution diluted by a featureless continuum, with the latter component described by a power law ($f_\nu \ \alpha \ \nu^\alpha$) with spectral index $\alpha = -1.5 \pm 0.5$. He estimated that the flux of the power law component extrapolated to ionizing energies was sufficient for generating the observed recombination line strengths. Given the uncertain details of Seyfert 2 continua, most photoionization calculations applied to these objects have represented the ionizing spectral energy by a power law. Typical best fit parameters for these calculations include: $\alpha = -1.5$; ionization parameter (the ratio of ionizing photon density to nuclear density at the face of a cloud) $u = 10^{-2}$ to $10^{-2.5}$; density $n_e \sim 10^3 \mathrm{cm}^{-3}$ and abundances $1/3$ - 1 solar. Kinney et al. (1991) found that the median value of the UV slope is $\alpha = -1.35$. These simple models succeed in reproducing the spectral features of Seyfert 2 galaxies only in a very broad sense. As the diagnostic diagrams of Veilleux & Osterbrock (1987) clearly show, there is considerable scatter around the theoretical predictions for Seyfert 2 galaxies. Ho et al. (1993b) showed that most of this dispersion arises from variations in the average heating energy per ionization, and hence the hardness of the photoionizing continuum (i.e., the ratio of X-ray to EUV fluxes). When the ionizing spectral energy distribution is parametrized as a power law, the observed line ratios are bracketed by variations of continuum spectral index spanning from $\alpha = -2.5$ to $\alpha = -1.0$. In fact, the actual energy distribution of the ionizing continuum may be quite different from that of a single power law (Binette et al., 1988). A more realistic model would consist of a power law spectrum plus a blackbody spectrum with temperature ranging from a few 10^4 K to a few 10^5 K (Stasinska, 1984; Robinson et al., 1987), which could be emitted by an accretion disk (Binette et al., 1988; Laor & Netzer, 1989; Fiore et al., 1995). Additional scatter may reflect intrinsic variation in the density, ionization parameter or abundances in the line-emitting gas. The nitrogen could be overabundant by a factor ~ 2 in at least some of the objects (Stasinska, 1984; Storchi-Bergmann & Pastoriza, 1989; Storchi-Bergmann, 1991; Cid Fernandez et al., 1992), while the heavy elements (oxygen and neon) could be depleted (Cruz-Gonzalez et al., 1991). There is a range of density in each of the objects; the strength of [OIII]λ4363 indicates electron densities ranging approximately from 10^4 cm^{-3} to 10^6 cm^{-3}, while the electron densities derived from [SII]λ6731/λ6716 are of the order of 10^3 cm^{-3} or less (Baldwin, 1975; Osterbrock, 1977; Bonatto & Pastoriza, 1990). Stasinska (1984) suggested that Seyfert 2 nuclei contain one system of high density clouds ($n_e > 10^6$ cm^{-3}) with roughly the same *u* ($\sim 10^{-2}$) for all objects, and one lower density cloud system ($n_e < 10^4$ cm^{-3}) for which *u* varies from one object to another.

Seyfert 1 galaxies show the presence of a cloud system with two well separated regions of line emission, the extended narrow-line region and the compact broad-line region, with a gap between the two with almost no line emission; this is naturally explained by the presence of dust mixed with the gas. The dust sublimes very close to the center where the velocity is high, giving rise to strong, broad emission lines. Dust absorption of ionizing photons dominates over gas absorption for large values of *u* ($> 10^{-2.2}$), introducing a gap with a significantly lower line emission efficiency from about $u \sim 0.1$ to about $\sim 10^{-2}$. Strong emission lines show up again below this value of *u*. Internal dust modifies the gas ionization and the line emission in several ways (Netzer & Laor, 1993). The chemical composition of the gas phase is modified by the heavy element depletion into the grains (Kingdom et al., 1995) which modifies the relative contribution of different elements to the cooling function and consequently changes various line intensity ratios of the emission-line spectrum (Shields, 1992).

2.3. Liners

According to Heckman's (1980) definition, Liners have $\lambda 3727 > \lambda 5007$, and $\lambda 6300 > 1/3 \ \lambda 5007$. The excitation mechanism of Liners has been highly controversial. Excitation mechanisms that have been proposed include photoionization by a dilute power-law continuum, shock heating, cooling flows, and photoionization by very hot Wolf-Rayet stars or normal O stars (see the review by Filippenko, 1993). Although Liners can best be explained by photoionization by non-stellar ionizing continua with a range of spectral hardness and gas densities, it cannot be excluded that at least some of these objects are shock heated (Moorwood et al., 1996) or photoionized by hot stars (Terlevich & Melnick, 1985; Filippenko & Terlevich, 1992; Schulz & Fritsch, 1994). Power-law models with a range in density $n_e = 10^{2.5} - 10^{5.5}$ cm^{-3}, ionization parameters $u = 10^{-3}$ to 10^{-4} and spectral index $\alpha = -2.5$ to -1 can reasonably reproduce the range of observed low-ionization line ratios of Liners (Ho et al., 1993b). In fact, the existence of a strong correlation between line width and critical density for de-excitation in the narrow-line region of some well studied Liners shows that the range of densities within each of these regions is very large ($n_e = 10^3 - 10^7$ cm^{-3}) (Filippenko & Halpern, 1984; Filippenko, 1985). Such conditions are probably common to most Liners as [OI]λ6300 is often found to be broader than each of the [SII]$\lambda\lambda$6716, 6731 lines (Filippenko & Sargent, 1985). The highest densities normally found in the narrow line region of Seyfert galaxies are a factor of ~ 10 smaller than the highest values found in Liners (Filippenko & Halpern, 1984).

Some Liners show a broad component of Hα (Keel, 1983a; Filippenko & Sargent, 1985; Ho et al., 1993a), a compact X-ray source (Koratkar et al., 1995), a compact ultraviolet nuclear emission (Maoz et al., 1995) and/or a compact radiocore (Heckman, 1980), which adds support to the hypothesis that they are genuine AGNs ionized by a non-stellar continuum.

2.4. Line widths

The forbidden emission lines in Seyfert galaxies are relatively broad; estimates of the FWHM median value range from 350 kms^{-1} (Vrtilek & Carleton, 1985; Whittle, 1985a; Wilson & Heckman, 1985) to 550 kms^{-1} (Heckman et al., 1981); this value may depend on the sample used, as the line width is correlated with the bulge luminosity of the galaxy, ranging from $\sim$ 400 kms^{-1} for Sbc galaxies to $\sim$ 700 kms^{-1} for ellipticals (Véron & Véron-Cetty, 1986). The emission line widths in Liners are comparable to those in narrow line regions of Seyfert galaxies (Heckman, 1980; Whittle, 1985a). The median FWHM for the [OIII] lines has been found to be smaller in Seyfert 1 galaxies ($\sim$ 380 kms^{-1}) than in Seyfert 2 ($\sim$ 500 kms^{-1}) (Heckman et al., 1981; Feldman et al., 1982; de Robertis & Osterbrock, 1986); this last result, however, has not been confirmed neither by Whittle (1985b), nor by Wilson & Heckman (1985). In radioquasars, the median FWHM of the [OIII] line is 520 kms^{-1} (Brotherton, 1996).

The emission line widths in nuclear HII regions and starburst galaxies are significantly smaller, with a median value of $\sim$ 160 kms^{-1} (Feldman et al., 1982; Brungardt, 1988). A limit to empirically dividing Seyfert galaxies from HII regions has been set to 300 kms^{-1} (Heckman et al., 1981; Shuder & Osterbrock, 1981), 250 kms^{-1} (Feldman et al., 1982; Whittle, 1985a) or even 150 kms^{-1} (Véron, 1981); there is however a substantial degree of overlap (Shuder & Osterbrock, 1981; Phillips et al., 1983; Whittle, 1985a; Wagner, 1988).

The line ratios and line widths being different in nuclear HII regions and in Liner and Seyfert nebulosities, the spectrum of the nuclear region of a galaxy in which both types of clouds are simultaneously present will have lines with different profiles (Heckman et al., 1983).

3. The composite spectra

3.1. Known AGNs having a composite spectrum

A number of objects having a composite spectrum are already known. They are listed in Table 1 and discussed below.

In **NGC 613**, line ratios measured by Osmer et al. (1974) indicate a "transition" spectrum. Observations around Hα with a resolution of $\sim$ 180 kms^{-1} show that it is a composite spectrum (Véron-Cetty & Véron, 1986b).

NGC 1275 is one of the original Seyfert galaxies (Seyfert, 1943). The relative [NII] intensity in the nucleus is low for a Seyfert-like object (Ho et al., 1993a); the [OII]λ3727 line is much narrower than the [OIII] lines (Balick & Heckman, 1979; Owen et al., 1996); the [OIII] and Hβ lines have different profiles; both lines appear to consist of two components: a narrow one (FWHM $\sim$ 400kms^{-1}) and a broad one (FWHM $\sim$ 2000 kms^{-1}); the narrower component is relatively more prominent in Hβ than in [OIII] (Heckman et al., 1981; Rosenblatt et al., 1994). In this object, the nucleus is surrounded by HII regions (Kent & Sargent, 1979); the narrow core of the lines is probably due to these HII regions, while the broader component arises in the high excitation gas in the Seyfert-like nucleus. The presence of weak, remarkably broad wings in the profile of Hα (Filippenko & Sargent, 1985) complicates the matter, but there is no doubt that NGC 1275 has a composite spectrum and that published line ratios cannot be used as diagnostic to determine the excitation mechanisms.

Mark 609 has a Seyfert 1.8 nucleus (Osterbrock, 1981); however, the Hβ profile is only 110 kms^{-1} wide, while the [OIII] lines are about 4 times wider ($\sim$ 450 kms^{-1}), suggesting the presence in the nuclear region of both a Seyfert nebulosity with $\lambda5007/H\beta \gg 5$ and a HII region with $\lambda5007/H\beta < 1$ (Heckman et al., 1981).

From their emission line ratios, **NGC 1672** and **NGC 6221** appear to be "transition" objects between Liners or Seyfert galaxies and HII regions (Osterbrock et al., 1992; Storchi-Bergmann et al., 1995); however, in both cases, λ5007 is much broader than Hβ (Véron et al., 1981b). In the case of NGC 6221, Véron-Cetty & Véron (1986b) have found in addition that the Hα and [NII] lines have two components, one with $\sim$ 200 kms^{-1} FWHM and $\lambda6584/H\alpha = 0.45$, the other with $\sim$ 580 kms^{-1} and $\lambda6584/H\alpha = 0.66$.

NGC 2782 is a galaxy which, although it belongs to the original list of Seyfert (1943), has been classified as a starburst galaxy by Sakka et al. (1973) and Kinney et al. (1984) on the basis of the nuclear emission line ratios; the [NII] and [SII] line strengths are however abnormally large for a HII region; medium resolution spectroscopy revealed that the Hβ and [OIII] lines have dramatically different profiles, with [OIII] showing both a broad core and high velocity wings (Kennicutt et al., 1989).

In the spectrum of the nucleus of **NGC 3367**, the emission lines are strong and broad (FWHM $\sim$ 490 kms^{-1} for Hβ); the line ratios are puzzling ($\lambda5007/H\beta = 0.50$, $\lambda6584/H\alpha = 0.87$, $\lambda6300/H\alpha = 0.05$) (Véron-Cetty & Véron, 1986b; Dekker et al., 1988; Ho et al., 1995). The Hα, [NII] complex, observed with a resolution of 180 kms^{-1} can be very well fitted by two sets of three Gaussian components with 240 and 640 kms^{-1} FWHM respectively (uncorrected for the instrumental broadening), having the same $\lambda6584/H\alpha$ ratio (0.87) (Véron-Cetty & Véron, 1986b). Further high resolution (160 kms^{-1}) observations around Hβ have shown that the [OIII] lines probably have the same profile as the [NII] lines, while Hβ has a narrow component (185 kms^{-1} FWHM, corrected for the instrumental profile) which could come from a HII region (Dekker et al., 1988); the corresponding Hα emission may not have been recognized due to unsufficient resolution.

NGC 4303 has been called a Liner by Huchra et al. (1982); Filippenko & Sargent (1985) showed that the nuclear spectrum is that of a HII region, each line, however, having a broad base suggesting the presence of a faint Seyfert 2 nucleus since, for these broad components, $\lambda6584/H\alpha > 1.0$. Véron-Cetty & Véron (1986b) have confirmed this diagnostic by finding that the Hα and [NII] lines have two components with widths equal to 180 and 400 kms^{-1} respectively; the narrow-line system has $\lambda6584/H\alpha = 0.43$, while the broad-line system has $\lambda6584/H\alpha = 3.21$. Moreover, in the nucleus, the λ5007 line is

Table 1. Known AGNs with a composite spectrum. This table gives for each object: the name (col. 1), the short position (col. 2), the Hubble type, taken from Sandage & Tammann (1981) for most galaxies, from Stockton (1968) for Mark 298, from MacKenty (1990) for Mark 609 and from Keel et al. (1985) for NGC 5953 (col. 3) and the published line intensities relative to Hβ (col. 4 to 8). The line fluxes have been corrected for internal and Galactic reddening using the standard Whitford (1958) law as tabulated by Lequeux et al. (1979). The amount of internal reddening was determined by comparing the observed Balmer decrement to an assumed intrinsic value Hα/Hβ = 3.1; there is indeed some evidence that the Balmer decrement in the narrow-line region of AGNs is near this value (Malkan, 1983; Jackson & Eracleous, 1995). This may indicate contributions either from collisional effects (Halpern & Steiner, 1983; Gaskell & Ferland,1984) or from dust mixed into the narrow-line region (Binette et al., 1994). References: (1) Ho et al. (1993a), (2) Ho et al. (1995), (3) Keel et al. (1985), (4) Kinney et al. (1984), (5) Koski (1978), (6) Osmer et al. (1974), (7) Osterbrock (1981), (8) Phillips et al. (1983), (9) Stauffer (1982), (10) Storchi-Bergmann et al. (1995).

Name	Short pos.	Hubble type	λ3727	λ5007	λ6300	Hα	λ6584	Ref.
NGC 613	0131 − 29	SBb	6.78	1.00	–	3.10	1.86	(6)
NGC 1275	0316 + 41	E pec	2.61	3.81	2.06	3.10	1.31	(1)
Mark 609	0322 − 06	Am.	1.82	5.22	0.28	3.10	2.85	(7)
NGC 1672	0444 − 59	S b	1.44	0.36	–	3.10	1.39	(10)
NGC 2782	0910 + 40	S a pec	4.31	1.34	–	3.10	1.76	(4)
NGC 3367	1043 + 14	SBc	–	0.37	0.15	3.10	2.81	(2)
NGC 4303	1219 + 04	S c	1.47	1.14	0.28	3.10	1.95	(9)
NGC 5953	1532 + 15	S a	5.56	2.84	0.35	3.10	3.82	(3)
Mark 298	1603 + 17	E pec	4.05	1.98	0.46	3.10	0.81	(5)
NGC 6221	1648 − 59	S bc	1.81	0.53	–	3.10	1.99	(10)
IC 5135	2145 − 35	S a pec	4.04	6.98	0.34	3.10	3.82	(8)
NGC 7496	2306 − 43	SBc	2.00	0.62	–	3.10	1.47	(10)
NGC 7582	2315 − 42	SBab	1.59	3.04	0.16	3.10	2.38	(10)

broad and strong, while the Hβ line is narrow and weak (Kennicutt et al., 1989).

The spectrum of the nucleus of **NGC 5953** cannot be easily classified from the emission-line ratios; however, out of the nucleus, the spectrum is similar to that of a HII region, suggesting that the emission line region is a composite of a HII and a Seyfert like cloud (Jenkins, 1984).

Mark 298 or IC 1182 has been variously classified as a Seyfert 2 galaxy (Koski, 1978; Khachikian & Weedman, 1974), a Liner (Dahari & de Robertis, 1988) or a HII region (Véron-Cetty & Véron, 1986a); it has a "transition" spectrum (Veilleux & Osterbrock, 1987). With a spectral resolution of 130 kms^{-1}, the Hβ and [OIII] lines show profiles which are definitely due to the superposition of several components that have different relative strengths of [OIII] to Hβ and that are kinematically and spatially distinct (Heckman et al., 1981).

In the case of **IC 5135**, although the optical emission line ratios in the nucleus are characteristic of Seyfert galaxies (Phillips et al., 1983; Storchi-Bergmann et al., 1995), the lines have profiles with two kinematic components, apparently resulting from a combination of relatively broad emission (FWHM $\sim$ 1000 kms^{-1}) from the Seyfert nucleus and narrow emission (FWHM $\sim$ 250 kms^{-1}) from low excitation, circumstellar HII regions (Shields and Filippenko, 1990).

NGC 7496 has a "transition" nuclear emission spectrum (Storchi-Bergmann et al., 1995). Observations of the Hβ spectral region with a resolution of 200 kms^{-1} show that the spectrum is composite (Véron et al., 1981a).

NGC 7582 has a "transition" nuclear emission spectrum (Ward et al., 1980; Storchi-Bergmann et al., 1995) which has been shown to be a composite spectrum by Véron et al. (1981a) and Véron-Cetty & Véron (1986b).

In addition, Kennicutt et al. (1989) have shown that many nuclear HII regions also contained a weak Liner or Seyfert cloud. Using optical spectrophotometry to compare the physical properties of HII regions located in galactic nuclei and in the disks, they have discovered that, in the diagram λ5007/Hβ *vs.* λ6584/Hα, the distributions of these two categories of objects are significantly different: while the disk HII regions define a narrow sequence, half of the nuclear regions have a larger value of λ6584/Hα for a given λ5007/Hβ. High dispersion spectra of a few of these objects show that, indeed, the line profiles are different, the [OIII] lines having a broad component which is absent or very weak in Hβ.

3.2. The narrow-line Seyfert 1 galaxies

A few galaxies have spectra very much like Seyfert 1 galaxies: strong blue continuum, strong FeII emission and weak forbidden lines; nevertheless, unlike Seyfert 1 galaxies, permitted and forbidden lines have almost the same width (Koski, 1978). Due to the presence of the unresolved "broad" Balmer components, these objects show, however, weak [OIII] , [NII] and [SII] lines when compared to the Seyfert 2 (Shuder & Osterbrock, 1981; Veilleux & Osterbrock, 1987), placing them out of the Seyfert 2 region in the emission-line diagnostic diagrams. When high signal-to-noise spectra are available, they are easily recognized because, although the ratio λ5007/Hβ is < 3, emission lines from FeII or higher ionization lines like [FeVII]λ6087 and [FeX]λ6375, are often present. The overwhelming evidence is that these objects are extensions of the Seyfert 1 class to low FWHM (Goodrich, 1989).

Table 2. This table gives for each of the observed objects: the name (col. 1), our spectral classification: S2: Seyfert 2, S1: Seyfert 1, C: composite spectrum (col. 2), the magnitude (col. 3) and the intensity of the main emission lines relative to Hβ (col. 4 to 8) taken from the reference given in col. 9. References: (1) de Grijp et al. (1992), (2) Fruscione & Griffiths (1991), (3) Keel et al. (1985), (4) Kim et al. (1995), (5) Lonsdale et al. (1992), (6) Osterbrock & de Robertis (1985), (7) Shuder & Osterbrock (1981), (8) Terlevich et al. (1991), (9) Véron-Cetty & Véron (1986a).

Name	Type	mag	λ3727	λ5007	λ6300	Hα	λ6584	Ref.
Mark 341	C	13.1	–	2.11	–	5.0	3.4	(3)
UM 85	?	17.	1.34	7.67	0.34	3.05	0.58	(8)
UM 103	S2	17.	2.88	10.29	0.54	3.27	1.28	(8)
MCG −02.05.022	C	15.8	–	2.90	–	3.48	1.44	(1)
IRAS 11058 − 1131	?	14.9	–	9.10	0.26	5.26	2.00	(6)
Mark 1361	C?	15.3	–	5.00	0.57	14.30	9.70	(4)
Mark 477	S1?	15.0	2.00	10.00	0.60	3.6	1.3	(7)
MCG 03.45.003	C	13.4	–	9.74	–	3.99	1.67	(1)
PGC 61548	C	14.2	–	1.29	0.39	3.10	2.14	(2)
IRAS 22017+0319	S2	15.4	–	9.29	–	3.81	1.82	(1)
ESO 602 − G25	C	14.3	–	1.11	0.67	11.10	7.44	(4)
Mark 308	C	14.6	–	4.8	0.3	5.8	2.3	(9)
NGC 7591	C	13.8	–	1.25	1.12	12.50	12.12	(4)
Mark 928W	C	13.6	–	2.84	0.70	7.76	5.10	(5)
IRAS 23365+3604	C	16.3	1.38	0.54	0.54	7.69	5.15	(4)

Examples of narrow-line Seyfert 1 galaxies which have been misclassified are:

Mark 507 (1748+68) which has been denied classification as a Seyfert by Shuder & Osterbrock (1981) and Osterbrock & Dahari (1983), and has been called a "transition" between a Liner and a Seyfert 2 by Heckman (1980). Halpern & Oke (1987) have however shown that the width of Hβ is clearly greater than that of [OIII]λ5007.

Mark 359 (0124+18), an SB0 galaxy (Huchra, 1977), was shown by Osterbrock & Pogge (1985) and MacAlpine et al. (1985) to have line ratios rather similar to those of a HII region. Davidson & Kinman (1978) and Veilleux (1991) were able to separate the broad and narrow components of the lines; the line ratios of the narrow line region are typical of Seyfert 2s.

Mark 1388 (1448+22) has been noticed by Veilleux & Osterbrock (1987) as being a Seyfert 2 galaxy with quite weak [SII] lines (and [NII] as well); its spectrum is unusual in having strong ionization lines and a strong featureless continuum, but narrow Balmer lines with essentially the same widths as the forbidden lines, combining characteristics found separately in Seyfert 1 and 2 galaxies (Osterbrock, 1985).

Baldwin et al. (1981), in their classification of extragalactic objects by their emission line spectra, concluded that **5C3.100** (Mark 957, 0039+40), as well as **Mark 42** (1151+46), an SBb galaxy (Adams, 1977), fall among the normal HII regions, suspecting however a combination of weak nuclear activity plus emission from normal HII regions. These objects are definitively narrow-line Seyfert 1 galaxies with strong FeII emission (Koski, 1978; Osterbrock & Pogge, 1985).

4. Observations and data analysis

4.1. Observations

We have chosen 15 emission line galaxies suspected to have composite spectra from their location in the Veilleux & Osterbrock (1987) diagnostic diagrams. They are listed in Table 2. Table 3 gives their optical positions measured on the Digitized Sky Survey[1] (Véron-Cetty & Véron, 1996). Eight of these objects are Seyfert 2 candidates ($\lambda5007/\mathrm{H}\beta > 3$) that show small [NII] relative intensities for this class ($\lambda6584/\mathrm{H}\alpha \leq 0.5$). The seven others have weak [OIII] lines ($\lambda5007/\mathrm{H}\beta < 3$) and relatively strong [NII] lines ($\lambda6584/\mathrm{H}\alpha > 0.65$), but the [OI] lines are weak, making their classification as Liners questionable.

Table 3. B1950 optical positions of the observed objects measured on the Digitized Sky Survey. The r.m.s. error is 0.6 arcsec in each coordinate; " * " indicates objects with larger errors because of their location near one edge of the Schmidt plate (Véron-Cetty & Véron, 1996).

Name	α	δ
Mark 341	00 34 13.90	23 42 36.5
UM 85	01 04 09.33	06 22 00.3*
UM 103	01 22 52.81	02 44 36.3
MCG −02.05.022	01 34 37.53	− 09 24 12.9
IRAS 11058 − 1131	11 05 49.65	− 11 31 56.8
Mark 1361	13 44 36.53	11 21 20.1
Mark 477	14 39 02.52	53 43 03.3
MCG 03.45.003	17 33 25.27	20 49 37.6*
PGC 61548	18 10 07.06	21 52 15.9
IRAS 22017+0319	22 01 47.32	03 19 17.0*
ESO 602 − G25	22 28 42.87	− 19 17 30.8
Mark 308	22 39 30.53	20 00 00.1
NGC 7591	23 15 43.88	06 18 44.7
Mark 928E	23 15 47.05	− 04 41 21.5
Mark 928W	23 15 47.34	− 04 41 24.4
IRAS 23365+3604	23 36 32.26	36 04 32.4

Spectroscopic observations were carried out from August 28 to Septembre 4, 1995 with the spectrograph CARELEC

[1] The Digitized Sky Survey was produced at the Space Telescope Science Institute (STScI) under U.S. Government grant NAG W-2166.

Table 4. Journal of observations. A: 66 Åmm^{-1} ($\lambda\lambda$6600-7500 Å), B: 66 Åmm^{-1} ($\lambda\lambda$4860-5760 Å). An " * " after the exposure time indicates the presence of clouds during the exposure.

Name	Disp.	Date 1995	Exp. time (min)
Mark 341	A	30.08	46*
	B	31.08	20
UM 85	A	28.08	20
	B	31.08	20
UM 103	A	28.08	20
	B	03.09	20
MCG −02.05.022	B	31.08	20
IRAS 11058 − 1131	A	21.03	20
Mark 1361	A	21.03	20
Mark 477	A	21.03	20
MCG 03.45.003	A	22.03	20
PGC 61548	B	02.09	20*
IRAS 22017+0319	A	28.08	20
	B	31.08	20
ESO 602 − G25	A	28.08	20
	B	01.09	20
Mark 308	B	31.08	20
NGC 7591	A	30.08	20*
	B	02.09	20
Mark 928W	A	28.08	20
	B	02.09	20
IRAS 23365 + 3604	A	28.08	20

(Lemaître et al., 1989) attached to the Cassegrain focus of the Observatoire de Haute Provence (OHP) 1.93m telescope. The detector was a 512 × 512 pixels, 27 × 27μm Tektronic CCD. From August 28 to 31, we used a 600 lmm^{-1} grating with a Schott GG 435 filter giving a 66 Åmm^{-1} dispersion in the range $\lambda\lambda$6700 − 7600 Å; from August 31 to September 4, we used the same grating in the blue, resulting in a 66 Åmm^{-1} dispersion in the range $\lambda\lambda$4860 − 5760 Å. In each case, the galaxy nucleus was centred on the slit. Usually five columns of the CCD ($\sim$ 5 arcsec) were extracted. The slit width was 2.1 arcsec, corresponding to a projected slit width on the detector of 52 μm or 1.9 pixel. The resolution, as measured on the night sky emission lines, was 3.4 Å FWHM. The red spectra have been flux calibrated using the standard stars BD 25°3941 (Stone, 1977) and BD 28°4211 (Oke, 1990); the blue spectra have been calibrated using Feige 15 (Stone, 1977) and BD 28°4211. Previous observations had been carried out from March 21 to 23, 1995 at 66 Åmm^{-1} in the range $\lambda\lambda$6500 − 7400 Å, using BD 26°2606 (Oke & Gunn, 1983) as a standard.

The journal of observations is given in Table 4.

4.2. Line profile fitting

The spectra were analysed in terms of Gaussian components as described in Véron et al. (1980; 1981a,c). The three emission lines, Hα and [NII]$\lambda\lambda$6548, 6584 (or Hβ and [OIII]$\lambda\lambda$4959, 5007) were fitted by one or several sets of three Gaussian components; the width and redshift of each component in a set were supposed to be the same and the intensity ratios of the [NII] and [OIII] lines were taken to be equal to 3 and 2.96, respectively (Osterbrock, 1974). When necessary, we have added an Hα or Hβ absorption component; as, usually, the Hα absorption line is completely filled up by the emission lines, we have assumed its intensity to be 1.8 times the intensity of the nearby absorption line of Ca I λ6495.4 (Véron-Cetty & Véron, 1986b). The result of this analysis is given in table 5.

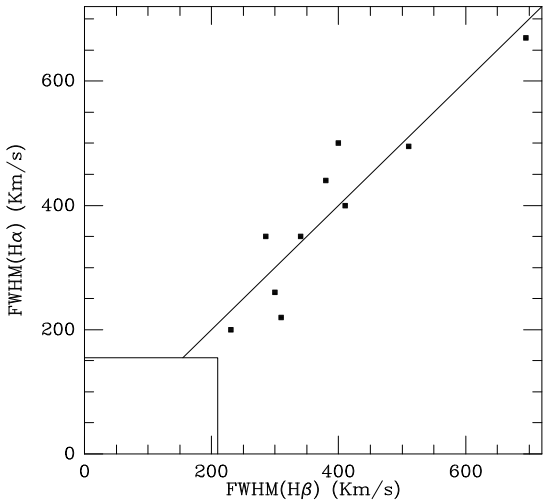

Fig. 1. Plot of the FWHM of the Hα *vs*. the FWHM of the Hβ systems. The FWHM are uncorrected for the instrumental broadening. The instrumental widths (155 kms $^{-1}$ at Hα, 210 kms $^{-1}$ at Hβ) are indicated. The good correlation between the two sets of measurements is an indication of the consistency of the fits.

Fig. 1 is a plot of the blue *vs*. the red FWHM for each system; the two widths are well correlated, showing the consistency of the decomposition of the lines into several Gaussian components. The velocity differences between the blue and red measurements of each set of observations is relatively small, never exceeding 75 kms^{-1}. There is however one exception: Mark 928W in which a "broad" component has been found in both the [OIII] and [NII] lines but with discrepant velocities and widths (Table 5).

4.3. Notes on individual objects

Mark 341 (IC 1559) is an S0 (de Vaucouleurs et al., 1979), or an E3 galaxy (Huchra, 1977). Its emission line spectrum has been studied by Keel et al. (1985). The observed line ratios (λ5007/Hβ = 2.11; λ6584/Hα = 0.68) suggest a Liner although λ6300 has not been detected. Our observations show that the spectrum is composite, with a "narrow" line cloud (210 kms^{-1} FWHM) with line ratios (λ5007/Hβ < 1.0; λ6584/Hα = 0.55) typical of a HII region and a "broad" line cloud (410 kms^{-1} FWHM) with line ratios: λ5007/Hβ > 5 and λ6584/Hα = 1.27) (Figs. 2, 4). The presence of a HII region in such an early type galaxy is rather surprising.

UM 85. Terlevich et al. (1991) have measured λ5007/Hβ = 7.67 and λ6584/Hα = 0.19, placing this object in an unlikely place in the λ5007/Hβ *vs*. λ6584/Hα diagram; we obtained

similar values: $\lambda5007/\mathrm{H}\beta$ = 6.53, $\lambda6584/\mathrm{H}\alpha$ = 0.20. All the lines are well represented by a Gaussian with FWHM = 400 kms^{-1}, broader than in most HII regions (Figs. 2, 4). This is a rather unusual object: the [NII] lines are too weak for a Seyfert galaxy and too strong for a HII region.

UM 103. The line ratios given by Terlevich et al. (1991) are $\lambda5007/\mathrm{H}\beta$ = 10.29 and $\lambda6584/\mathrm{H}\alpha$ = 0.39. Our best fits involve two sets of components, both having line ratios typical of Seyfert 2s; the $\lambda6584/\mathrm{H}\alpha$ ratios (0.54 and 0.57) are significantly larger than the published value (Figs. 2, 4). $\lambda6300$ is also present with an intensity about 16% Hα. If our estimate of the [NII] line relative intensity is correct, this object is a Seyfert 2 galaxy with normal relative line intensities.

MCG −02.05.022 is a Seyfert 2 according to de Grijp et al. (1992); however, their published spectrum shows relatively weak [OIII] and [NII] lines ($\lambda5007/\mathrm{H}\beta$ = 2.90, $\lambda6584/\mathrm{H}\alpha$ = 0.41). Our spectrum ($\lambda\lambda4900-5600$ Å) shows relatively broad, asymmetrical [OIII] lines and a much narrower Hβ emission line. The best fit is obtained with a narrow set of Gaussian components, with FWHM = 370 kms^{-1} and $\lambda5007/\mathrm{H}\beta$ = 1.38 plus a broad set of components with FWHM = 1150 kms^{-1} and $\lambda5007/\mathrm{H}\beta > 10$ (Fig. 4). This spectrum is therefore composite with a HII region and a Seyfert 2 cloud.

IRAS 11058−1131 has been classified as a Seyfert 2 galaxy by de Grijp et al. (1992) and Osterbrock & de Robertis (1985). Young et al. (1993) have reported the presence of very strong, broad Hα emission (FWHM $\sim$ 7600 kms^{-1}) in the polarized flux spectrum. Osterbrock & de Robertis (1985) have remarked that the emission lines are very narrow (FWHM $<$ 250 kms^{-1}); they have measured line ratios unusual for a Seyfert 2 galaxy: $\lambda5007/\mathrm{H}\beta$ = 9.10 and $\lambda6584/\mathrm{H}\alpha$ = 0.38. Our spectrum confirms the low relative intensity of the [NII] lines ($\lambda6584/\mathrm{H}\alpha$ = 0.36); $\lambda6300$ is observed with an intensity $\sim$ 5% Hα. Our best fit results from using two sets of Gaussian components with FWHM = 200 and 325 kms^{-1} respectively, but both have weak [NII] lines ($\lambda6584/\mathrm{H}\alpha$ = 0.28 and 0.44 respectively) (Fig. 2). The nature of this spectrum is still unclear; however, it seems possible that the relative intensities of the various components given by the fitting procedure are affected by large errors, the redshifts and widths of the two emission line systems being not very different.

Mark 1361 (IRAS 13446+1121) is a Seyfert 2 galaxy according to Kim et al. (1995), with $\lambda5007/\mathrm{H}\beta$ = 5 and $\lambda6584/\mathrm{H}\alpha$ = 0.33; the low [NII] relative intensity is probably due to a misprint as the published spectrum shows a much larger $\lambda6584$ relative intensity. Our spectrum indeed shows a relatively strong $\lambda6584$ line. The Hα and [NII] lines have been fitted by two sets of Gaussian components with widths of 305 and 420 kms^{-1} FWHM respectively and line ratios $\lambda6584/\mathrm{H}\alpha$ = 0.69 and 1.35; the "broad-line" system is blueshifted by 336 kms^{-1} with respect to the "narrow-line" system (Fig. 2); it is most likely due to a Seyfert cloud. A high-resolution spectrum of the Hβ and [OIII] lines is needed before concluding that the "narrow-line" region is a HII region.

Mark 477 (I Zw 92) has a very high ionization emission-line spectrum with [NeV]$\lambda3426$, HeII$\lambda4686$, [FeVII]$\lambda6087$ and [FeX]$\lambda6375$ and an almost completely non stellar variable continuum; the [OIII] lines are strong ($\lambda5007/\mathrm{H}\beta$ = 11.8), while the [NII] lines are relatively weak ($\lambda6584/\mathrm{H}\alpha$ = 0.28) (Kunth & Sargent, 1979; Shuder & Osterbrock, 1981; de Robertis & Osterbrock, 1986; de Robertis, 1987; Veilleux, 1988; Kinney et al., 1991; McQuade et al., 1995). De Robertis & Osterbrock (1986) have remarked that these properties make this object very similar to narrow-line Seyfert 1 galaxies. However, Hubble Space Telescope observations have not revealed the presence of an unresolved nucleus (Nelson et al. 1996). Our best fit consists of two sets of three Gaussian components and a broad Hα component ($\sim$ 1850 kms^{-1} FWHM) (Fig. 2); the relative intensity of the [NII] line is small in both emission line systems ($\lambda6584/\mathrm{H}\alpha \sim 0.34$), while we expected the "broad-line" system to be dominated by the "narrow" Seyfert 1 Balmer component and the narrow-line system to be Seyfert 2-like, with strong relative [NII] lines. Tran et al. (1992) and Tran (1995) have detected weak broad (FWHM $\sim$ 3100 kms^{-1}) polarized permitted Balmer lines in the spectrum of Mark 477. The nature of this object is unclear; the similarity of the Hα and [NII] profiles is puzzling. Again, high-spectral resolution for the Hβ and [OIII] lines could help understanding it.

MCG 03.45.003 (IRAS 17334+2049) has been classified as a Seyfert 2 galaxy by de Grijp et al. (1992) on the basis of the strong [OIII] line ($\lambda5007/\mathrm{H}\beta$ = 9.74); however, the [NII] lines are rather weak ($\lambda6584/\mathrm{H}\alpha$ = 0.42). The Hα and [NII] lines were fitted on our spectrum by two sets of three Gaussian components with widths of 190 and 430 kms^{-1} FWHM (the narrow component is in fact unresolved), the line ratios being $\lambda6584/\mathrm{H}\alpha$ = 0.47 and 0.61 respectively. The "broad" line system is blue shifted by 42 kms^{-1} with respect to the "narrow" line system (Fig. 3). It is probably a composite spectrum with a "narrow-line" HII region and a "broad-line" Seyfert 2 cloud. This should be confirmed by high resolution observations of the Hβ and [OIII] lines.

PGC 61548 has been classified as an AGN by Fruscione & Griffiths (1991), with $\lambda5007/\mathrm{H}\beta$ = 1.29, $\lambda6584/\mathrm{H}\alpha$ = 0.69 and $\lambda6300/\mathrm{H}\alpha$ = 0.12. Our blue spectrum clearly shows a composite nature, with Hβ much narrower than [OIII] (Fig. 4).

IRAS 22017+0319 is an elliptical (Hutchings & Neff, 1991) Seyfert 2 galaxy (Hill et al., 1988; de Grijp et al., 1992). The line ratios are: $\lambda5007/\mathrm{H}\beta$ = 9.29, $\lambda6584/\mathrm{H}\alpha$ = 0.48 (de Grijp et al., 1992), placing this object at the limit of the Seyfert 2 distribution. Our data (Figs. 3, 5) show the spectrum to be composite with a "narrow" line cloud (FWHM $\sim$ 280 kms^{-1}) having $\lambda5007/\mathrm{H}\beta$ = 9.60, $\lambda6584/\mathrm{H}\alpha$ = 0.52, and a "broad" line cloud (FWHM $\sim$ 680 kms^{-1}) having $\lambda5007/\mathrm{H}\beta$ = 10.1, $\lambda6584/\mathrm{H}\alpha$ = 0.49. The two clouds have almost identical line ratios; this is therefore a Seyfert 2 galaxy with complex line profiles rather than a composite spectrum. The redshift is z = 0.066 according to Hill et al. (1988) and z = 0.0611 according to de Grijp et al. (1992); our value is z = 0.0658.

ESO 602 − G25. The line ratios in this object are $\lambda5007/\mathrm{H}\beta$ = 1.10 and $\lambda6584/\mathrm{H}\alpha$ = 0.67 (Kim et al., 1995); these values are rather atypical; moreover $\lambda6300$ is rather low

Table 5. Fitting profile analysis results. Col. 1 gives the name of the object, col. 2 the adopted redshift, col. 3 and 7 the velocities for each set of components measured on the blue and red spectra, respectively, and deredshifted using the redshift given in col. 2; col. 4 and 8 the corresponding FWHM (uncorrected for instrumental broadening), col. 5 and 9, the intensity ratios $\lambda5007/\mathrm{H}\beta$ and $\lambda6584/\mathrm{H}\alpha$ respectively and col. 6 and 10 the fraction of the flux of Hβ emission (respectively Hα) in each component with respect to the total flux of the line in each object. Col. 11 is the velocity difference between the blue and red systems.

Name	z	V	FWHM	$\frac{\lambda5007}{\mathrm{H}\beta}$	Hβ	V	FWHM	$\frac{\lambda6584}{\mathrm{H}\alpha}$	Hα	ΔV
		(kms^{-1})	(kms^{-1})		(%)	(kms^{-1})	(kms^{-1})		(%)	(kms^{-1})
Mark 341	0.017	−56	230	$< 1.$	100	−38	200	0.55	53	−18
		−28	380	$> 5.$	–	−67	440	1.27	47	39
UM 85	0.041	−26	410	6.53	100	−58	400	0.20	100	32
UM 103	0.045	−29	310	6.7	75	−23	220	0.54	51	−6
		−190	510	16.0	25	−117	495	0.57	49	−73
MCG −02.05.022	0.070	6	370	1.38	100	–	–	–	–	–
		−256	1150	> 10.0	–	–	–	–	–	–
IRAS 11058 − 1131	0.055	–	–	–	–	−61	200	0.28	43	–
		–	–	–	–	−1	325	0.44	57	–
Mark 1361	0.023	–	–	–	–	−43	305	0.69	90	–
		–	–	–	–	−370	420	1.35	10	–
Mark 477	0.038	–	–	–	–	−44	200	0.34	20	–
		–	–	–	–	−19	430	0.33	40	–
		–	–	–	–	−46	1850	–	40	–
MCG 03.45.003	0.024	–	–	–	–	−25	190	0.47	52	–
		–	–	–	–	−67	430	0.61	48	–
PGC 61548	0.018	−94	285	< 0.1	100	–	–	–	–	–
		−132	370	> 10.0	–	–	–	–	–	–
		−263	540	> 5.0	–	–	–	–	–	–
IRAS 22017+0319	0.066	−33	300	9.6	68	−65	260	0.52	67	32
		−145	695	10.1	32	−180	670	0.49	33	35
ESO 602−G25	0.025	24	285	0.23	81	−17	350	0.51	96	41
		−268	340	9.1	19	−343	350	2.67	4	75
Mark 308	0.024	−210	170	< 0.3	48	–	–	–	–	–
		−110	230	10.2	31	–	–	–	–	–
		−170	725	10.2	21	–	–	–	–	–
NGC 7591	0.017	–	–	–	–	−196	180	0.46	26	–
		–	–	–	–	−70	430	1.28	74	–
Mark 928W	0.024	−103	300	0.99	100	−172	190	0.41	–	−69
		96	400	$> 7.$	–	−60	285	1.04	–	156
		315	1260	$> 7.$	–	−44	610	–	–	–
IRAS 23365+3604	0.064	–	–	–	–	−30	240	0.46	81	–
		–	–	–	–	−152	525	1.70	19	–

(6% Hα). Our spectra (Figs. 3, 5) clearly show two clouds with a velocity difference of $\sim$ 310 kms^{-1}. The two clouds have about the same line width ($\sim$ 330 kms^{-1} FWHM), but their line ratios are quite different. The high velocity cloud has $\lambda6584/\mathrm{H}\alpha$ = 0.51 and $\lambda5007/\mathrm{H}\beta$ = 0.23, typical values for a low excitation HII region, while the low velocity cloud has line ratios $\lambda6584/\mathrm{H}\alpha$ = 2.67 and $\lambda5007/\mathrm{H}\beta$ = 9.1, that are typical of Seyfert 2s.

Mark 308 is a Seyfert 2 galaxy according to Popov & Khachikian (1980) and Zamorano et al. (1994). However, Véron-Cetty & Véron (1986a) stated that it is an high excitation HII region, the line ratios being: $\lambda5007/\mathrm{H}\beta$ = 4.8, $\lambda6584/\mathrm{H}\alpha$ = 0.40; such values are unlikely for a HII region and for a Seyfert galaxy either. Our high dispersion spectrum, including Hβ and λ5007, reveals a composite spectrum (Fig. 5).

NGC 7591, an SBbc galaxy (de Vaucouleurs et al., 1991), has been classified as a Liner by Kim et al. (1995). The Balmer decrement of the nuclear emission region is very high ($\mathrm{H}\alpha/\mathrm{H}\beta$ = 12.3); as a result Hβ is very weak and difficult to measure. In addition, λ6300 is rather weak for a Liner ($\lambda6300/\lambda5007$ = 0.31). From our data, we have found the Hα and [NII] lines to be composite. One system has a line width of 180 kms^{-1} FWHM with $\lambda6584/\mathrm{H}\alpha$ = 0.46, while the other has a line width of 430 kms^{-1} and $\lambda6584/\mathrm{H}\alpha$ = 1.28 (Fig. 3). The low signal-to-noise ratio of the blue spectrum does not allow to make the same analysis for the Hβ and [OIII] lines.

Mark 928W. Mark 928 or NGC 7592 is the interactive system VV 731 (Vorontsov-Velyaminov, 1977), well illustrated by Mazzarella & Boroson (1993). The western component has been classified as a Seyfert 2 galaxy by Arkhipova et al. (1981), Denisyuk & Lipovetski (1983) and Mazzarella & Boroson (1993). However, for Dahari (1985), it is a marginal Seyfert

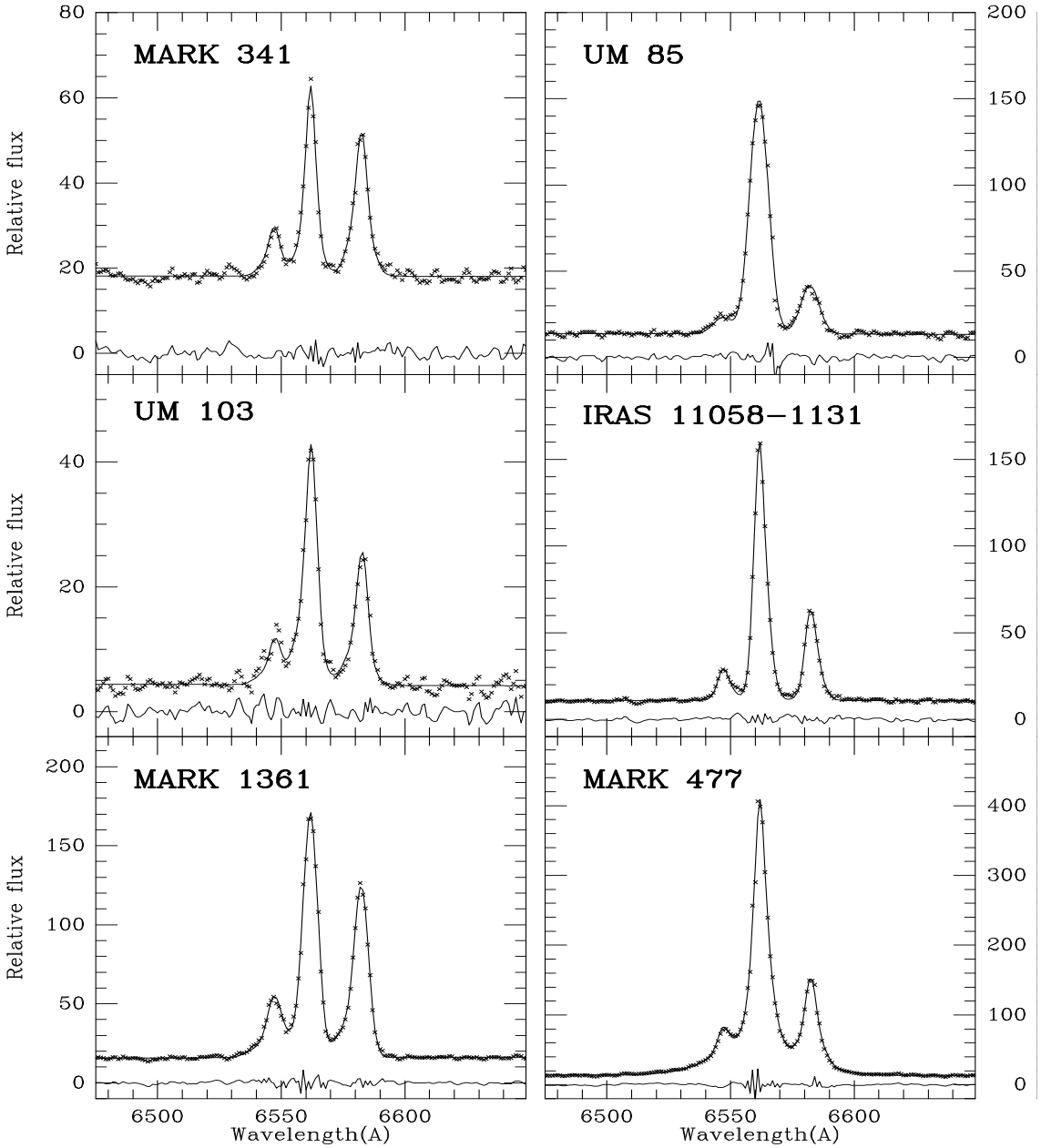

Fig. 2. High dispersion spectra (resolution $\sim$ 3.4 Å) of the Hα, [NII] complex for six of the program objects. The solid line is the best fit with Gaussian components (see text). The lower line shows the residuals (differences between observations and model).

or a Seyfert/Liner because of the low value of the $\lambda5007/\mathrm{H}\beta$ ratio ($\sim$ 3). Lonsdale et al. (1992) have published line ratios for this object: $\lambda5007/\mathrm{H}\beta$ = 2.84, $\lambda6584/\mathrm{H}\alpha$ = 0.66, $\lambda6300/\mathrm{H}\alpha$ = 0.10, making it a rather marginal object. Our spectra (Figs. 3, 5) clearly show the presence of a HII region (FWHM $\sim$ 250 kms^{-1}, $\lambda5007/\mathrm{H}\beta$ = 0.99, $\lambda6584/\mathrm{H}\alpha$ = 0.41) and of a Seyfert 2 nebulosity (FWHM $\sim$ 340 kms^{-1}, $\lambda5007/\mathrm{H}\beta > 7$, $\lambda6584/\mathrm{H}\alpha$ = 1.04). A third component is needed to obtain good fits; however, the velocity and width of this third component are significantly different for the blue and red spectra (Table 5); this is not understood. Mark 928E is a pure HII region, with FWHM $\sim$ 280 kms^{-1}, $\lambda5007/\mathrm{H}\beta$ = 0.67, $\lambda6584/\mathrm{H}\alpha$ = 0.33. It had been called a HII region by Dahari & de Robertis (1988) and a Liner by Mazzarella & Boroson (1993).

IRAS 23365+3604. Low dispersion spectra have been published by Klaas & Elsasser (1991) and Kim et al. (1995). No unambiguous classification is possible for this object from the line ratios ($\lambda5007/\mathrm{H}\beta$ = 1.5, $\lambda6584/\mathrm{H}\alpha$ = 0.64, $\lambda6300/\mathrm{H}\alpha$ = 0.13), but the spectrum can be reproduced if an extreme Liner spectrum contributes 60% and a HII region spectrum 40% (Klaas & Elsasser, 1991). Our spectrum best fit (Fig. 3) is obtained with two sets of Gaussian profiles with FWHM equal to 240 and 525 kms^{-1} and line ratios $\lambda6584/\mathrm{H}\alpha$ = 0.46 and 1.70 respectively; this confirms that this object has a composite

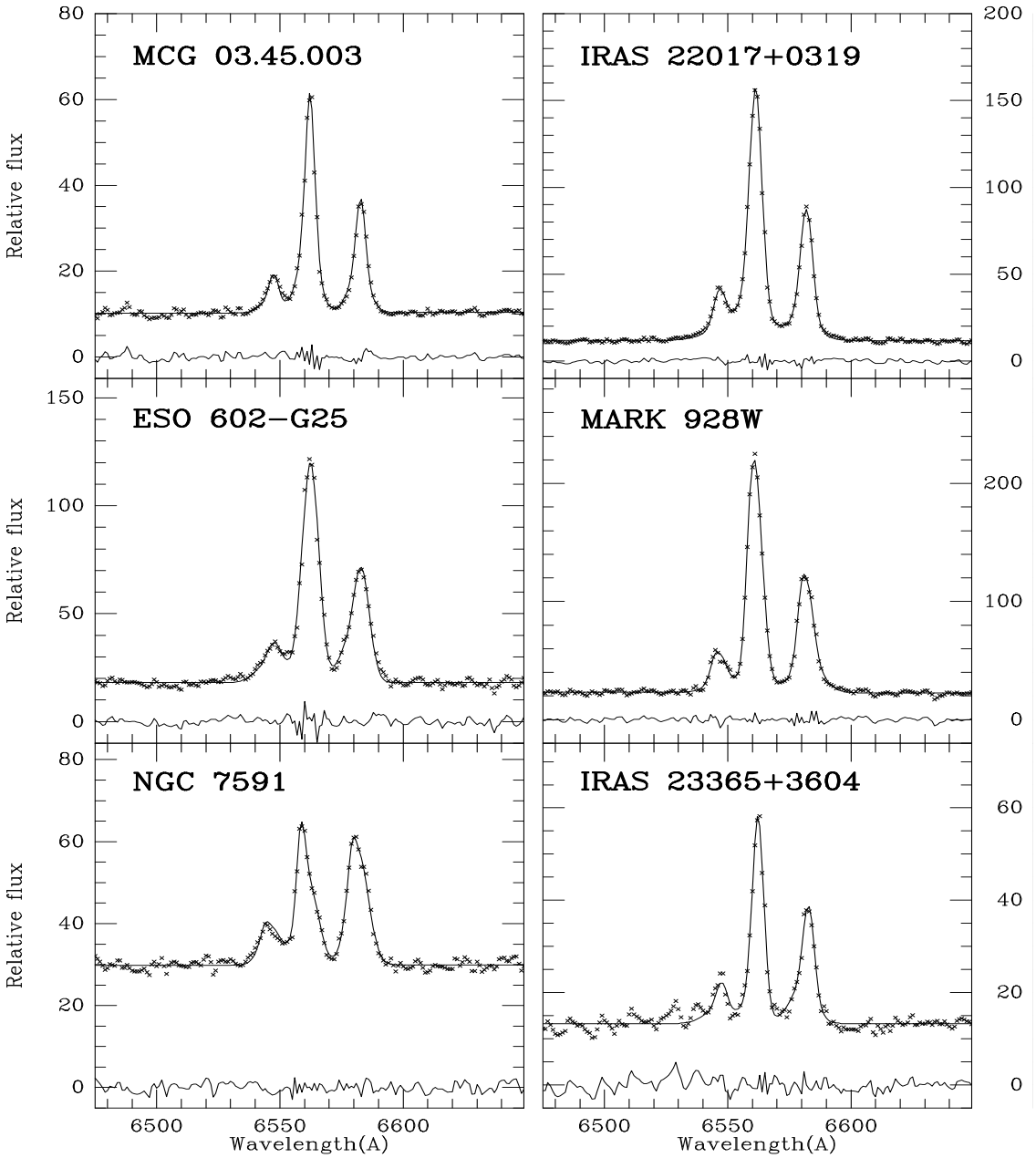

Fig. 3. High dispersion spectra (resolution $\sim$ 3.4 Å) of the Hα, [NII] complex for six of the program objects. The solid line is the best fit with Gaussian components (see text). The lower line shows the residuals (differences between observations and model).

spectrum. The strength of the [OI] lines (13% of the total Hα flux), suggests that this "broad-line" component could indeed be a Liner rather than a Seyfert 2 cloud. High resolution spectroscopy of the Hβ and [OIII] lines is needed to confirm this hypothesis. These observations could be made difficult by the large observed reddening (Hα/Hβ = 17.85). Klaas & Elsasser (1991) have found some evidence for a broad ($\sim$ 1500 kms^{-1} FWHM) Hα component; there is no hint of such a broad Hα line in our spectrum.

5. Results

Two objects (UM 103 and IRAS 22017+0319) turned out to be pure Seyfert 2 with marginally low [NII] lines; one (IRAS 11058 − 1131) requires more observations before drawing any conclusion; ten have a composite spectrum with a HII region and a Seyfert-like nucleus projected on the spectrograph aperture; their measured relative line intensities cannot be used in the diagnostic diagrams; one object (Mark 477) is probably a narrow line Seyfert 1 galaxy. The most interesting object is UM 85 in which all lines have, at our resolution, the same profile and redshift, although the spectrum is really intermediate, with the

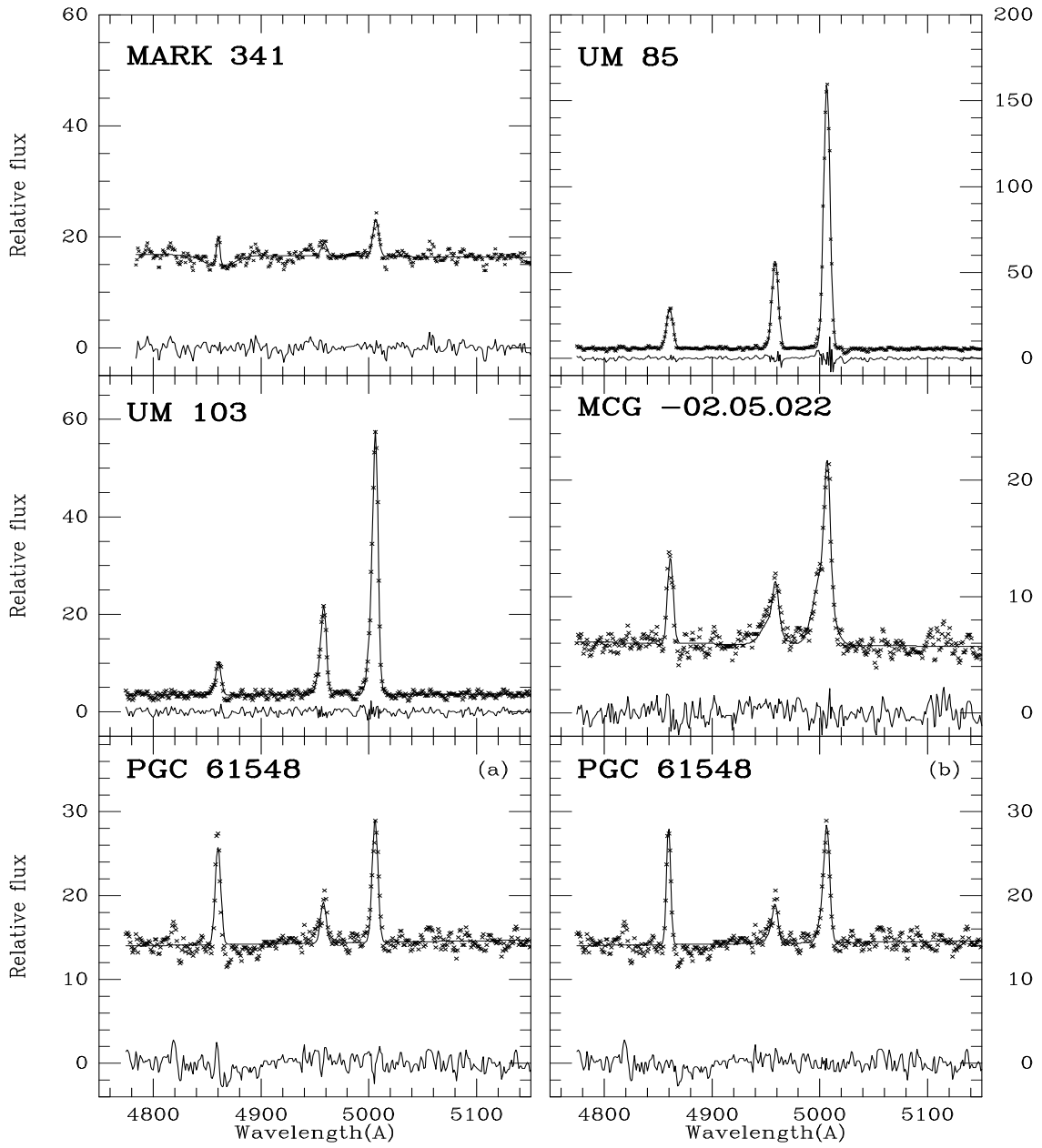

Fig. 4. High dispersion spectra (resolution $\sim$ 3.4 Å) of the Hβ, [OIII] complex for five of the program objects. The solid line is the best fit with Gaussian components. For PGC 61548 we also give the unsatisfactory fit with a single set of three Gaussian components (a). The lower line shows the residuals (differences between observations and model).

[NII] lines too strong for a HII region and too weak for a Seyfert galaxy ($\lambda6584/\mathrm{H}\alpha$ = 0.20), at the observed $\lambda5007/\mathrm{H}\beta$ ratio (6.53).

We have found in the literature two additional objects which, in the present state of the published observations, seem to be genuine "transition" objects: the radiosource **3C 184.1** (0734+80) has been identified with a 17.0 mag galaxy (Whyndam, 1966) at z = 0.118 (Simkim, 1979); it is a normal giant elliptical (Owen & Laing, 1989). The radiocore accurately coincides with the galaxy (Riley & Pooley, 1975). A radio map published by Leahy & Perley (1991) shows that it is a FR II radiogalaxy in the classification scheme of Fanaroff & Riley (1974). Spectrophotometry of this object has been carried out by Koski (1978): $\lambda5007/\mathrm{H}\beta$ = 11.08 and $\lambda6584/\mathrm{H}\alpha$ = 0.22. It is very unlikely that a normal giant elliptical radiogalaxy would contain a HII region and that the spectrum of 3C 184.1 would be composite. It could be that this object is a narrow-line Seyfert 1 galaxy; high resolution observations of the Hα, [NII] complex could show that the Hα and [NII] lines don't have the same profile.

3C 198.0 (0819+06) has been identified with a 17.0-17.4 elliptical galaxy (Clarke et al., 1966; Wyndham, 1966) at z = 0.0815 (Schmidt, 1965); it is the brightest member of a loose

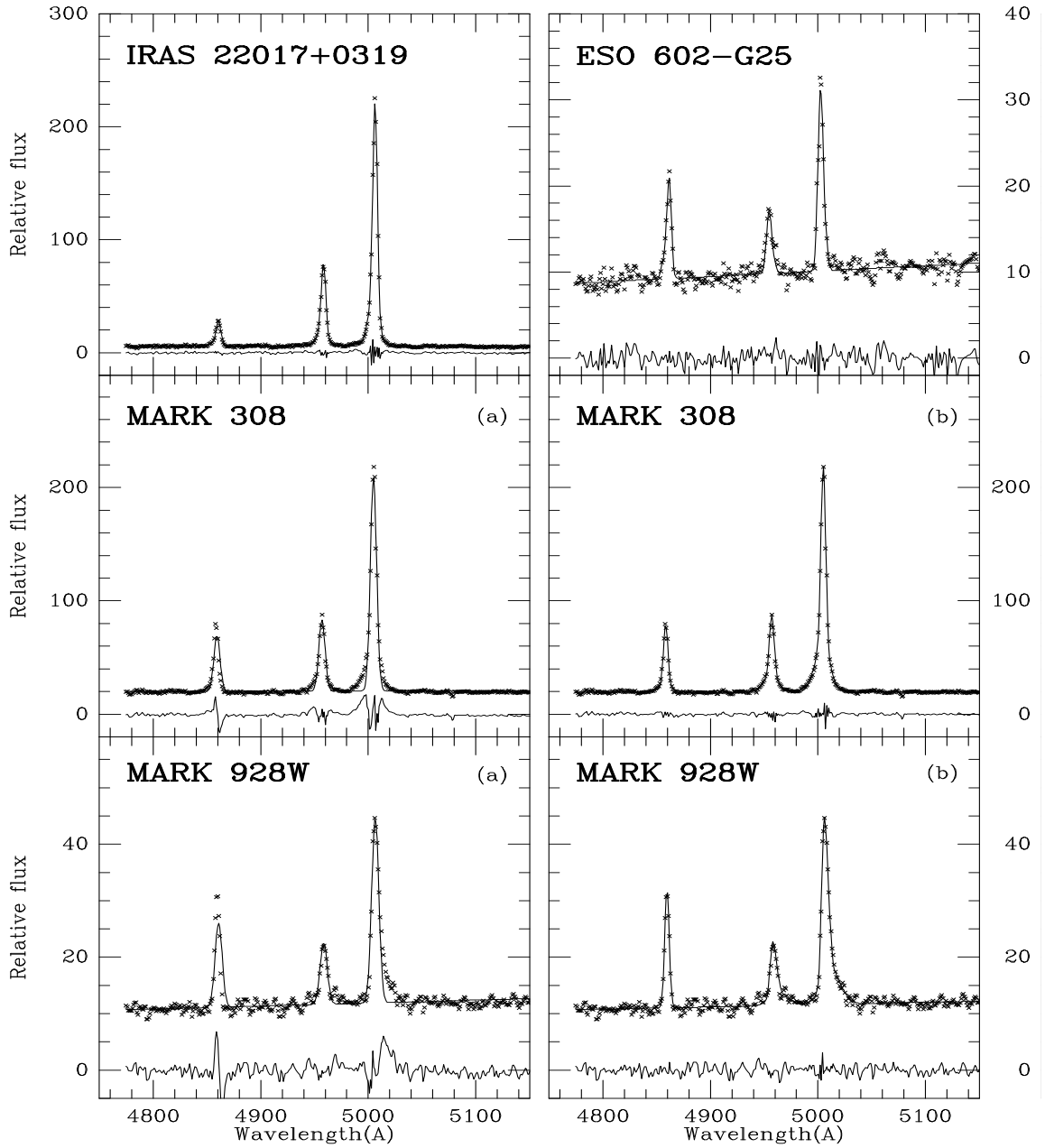

Fig. 5. High dispersion spectra (resolution $\sim$ 3.4 Å) of the Hβ, [OIII] complex for four of the program objects. The solid line is the best fit with Gaussian components. For Mark 308 and Mark 928W, we also give the unsatisfactory fit with a single set of Gaussian components (a). The lower line shows the residuals (differences between observations and model).

cluster of galaxies (Maltby et al., 1962). The main body of the galaxy is blue relatively to a giant elliptical at its redshift; it contains a nuclear point source which is even bluer than the parent galaxy (Smith & Heckman, 1989). A relatively strong nuclear nonthermal component is present (Yee & Oke, 1978). It is a FR II radiogalaxy, although the only published radiomap is rather crude (Fomalont, 1971). The line ratios (Cohen & Osterbrock, 1981) are those of a HII region which is extremely surprising in an elliptical radiogalaxy.

6. Conclusions

In Fig. 6a–d we give two of the Veilleux & Osterbrock (1987) diagnostic diagrams built from a compilation of spectrophotometric data of 1245 emission-line nuclei published in more than 140 papers, excluding known Seyfert 1, 1.8 or 1.9 galaxies. Fig. 6a gives $\lambda5007/\mathrm{H}\beta$ *vs.* $\lambda6584/\mathrm{H}\alpha$ for HII regions, Seyfert 2 galaxies and Liners; the three classes are well separated as is well known. Fig. 6c shows the same diagrams for the objects with composite spectra and for those with an ambiguous "transition" spectrum. Figs. 6b and 6d are similar but for the line ratios $\lambda5007/\mathrm{H}\beta$ *vs.* $\lambda6300/\mathrm{H}\alpha$.

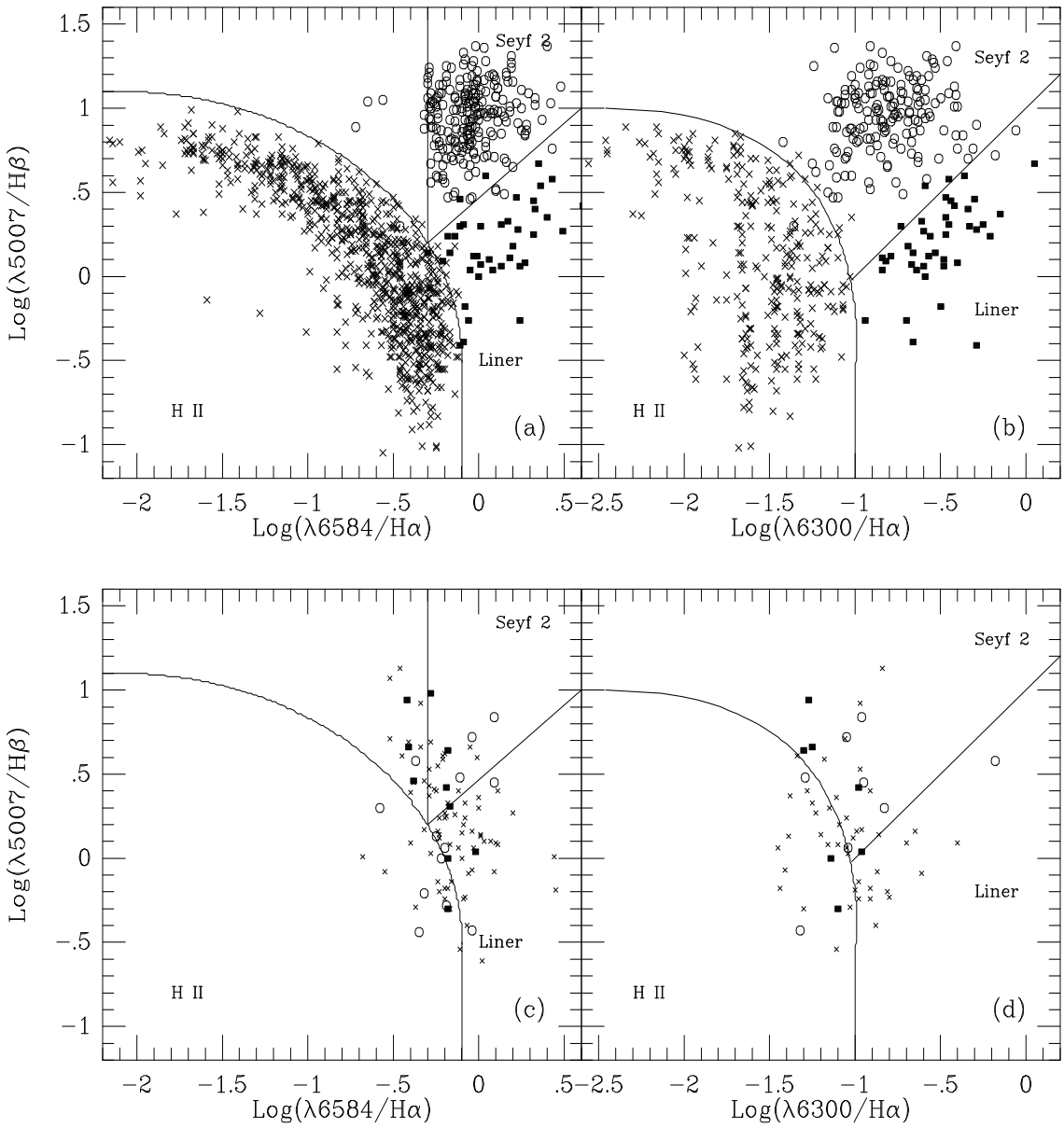

Fig. 6a–d. The upper panel is a plot of the logarithm of the dereddened measured line ratios ($\lambda5007/\mathrm{H}\beta$ *vs.* $\lambda6584/\mathrm{H}\alpha$ and $\lambda5007/\mathrm{H}\beta$ *vs.* $\lambda6300/\mathrm{H}\alpha$) for HII regions (crosses), Liners (squares) and Seyfert 2 (circles) compiled from the literature. The three classes of objects are well segregated in these diagrams. The classification adopted here for each object is taken from the literature and is usually based on the use of diagnostic diagrams. The lower panel show the same plot, but for the unclassified objects (crosses), for the composite spectra collected from the literature (empty circles) and for the composite spectra from this paper (filled squares).

The lines separating the various classes of objects in Fig. 6 are arbitrary, except for the line separating Seyfert 2s and Liners (Figs. 6b and 6d) which corresponds to [OI]$\lambda6300$ = 0.33[OIII]$\lambda5007$, the original dividing line proposed by Heckman (1980). The line separating Seyfert 2s and Liners in Figs. 6a and 6c seems to be more effective than the generally adopted limit ([OIII]$\lambda5007$ = 3Hβ) in achieving the same separation between the two classes, as examination of Fig. 6a shows.

The fact that only one (UM 85) of the 15 transition objects taken from this hopefully complete compilation seems to have a genuine transition spectrum indicates that HII regions, Seyfert 2 galaxies and Liners fall into well defined, clearly separated regions in the diagnostic diagrams. However, the presence of a few objects in the "forbidden" region of Fig. 6a (at $\lambda5007/\mathrm{H}\beta \sim 10$, $\lambda6584/\mathrm{H}\alpha \sim 0.25$) deserves attention.

Seyfert 2 galaxies are clustered in a relatively small volume in the three-dimensional space $\lambda5007/\mathrm{H}\beta$, $\lambda6584/\mathrm{H}\alpha$, $\lambda6300/\mathrm{H}\alpha$. In particular, there is a sharp limit at $\lambda6584/\mathrm{H}\alpha$ = 0.5 below which no Seyfert 2s are found (we have found in the literature a dozen objects classified as Seyfert 2 with $\lambda6584/\mathrm{H}\alpha < 0.5$ (Fig. 6c); the four which have been observed

with sufficient spectral resolution are composite); the existence of this limit is not predicted by the ionization models.

Our sample of objects, although large, is not complete in any sense; however, it seems to suggest that Seyfert 2s and Liners occupy distinct regions of the line ratio space rather than constituting a continuum which would probably be expected if these two classes of objects differ only by the value of their ionization parameter.

We have seen above that Kennicutt et al. (1989) have shown that nuclear HII regions occupy a broader sequence than the disk HII regions in the $\lambda5007/\mathrm{H}\beta$ *vs.* $\lambda6584/\mathrm{H}\alpha$ diagram, suggesting the presence of a weak Seyfert-like nebulosity. Similarly Seyfert or Liner spectra may be affected by the presence of a weak HII region. Seyfert-like nebulosities, being usually more centrally concentrated that HII regions, the degree of pollution of the nuclear spectra by HII regions will increase with the aperture of the slit and the distance of the galaxy (aperture effects have been discussed by Ho et al., 1993b). Observations with better spectral resolution and higher signal-to-noise ratio than those achieved in this paper could allow to analyse these spectra. But the net result of such an analysis would be to reduce even more the area occupied by each class of objects in the diagnostic diagrams.

Some objects which do not meet Heckman's (1980) criteria for Liners, but which have been classified as Liners by other authors based on other criteria, most commonly a high value of $\lambda6584/\mathrm{H}\alpha$ (> 0.6), have a low value of $\lambda6300/\mathrm{H}\alpha$ ($< 1/6$). They are called "weak-[OI] Liners". The simplest interpretation of their spectral characteristics is that they are composite HII region/Liner systems - that is, either nebulae which are excited by hot stars and by non stellar radiation, or mixtures of normal HII regions and nebulae excited by non stellar radiation (Ho et al., 1993a). It is also possible to model the optical spectral properties of these objects with photoionization by very hot O-type stars alone (Filippenko & Terlevich, 1992). High resolution spectral observations should be made to settle the question.

In Fig. 6b, there is a number of Seyfert 2s with relatively low $\lambda5007$ and $\lambda6300$ emission lines ($\lambda5007/\mathrm{H}\beta \sim 3$, $\lambda6300/\mathrm{H}\alpha \sim 0.06$); they should also be observed to check for the possible presence of a nuclear HII region.

Acknowledgements. This research has made use of the NASA/IPAC extragalactic database (NED) which is operated by the Jet Propulsion Laboratory, Caltech, under contract with the National Aeronautics and Space Administration. A. C. Gonçalves acknowledges support from the JNICT during the course of this work, in the form of a PRAXIS XXI PhD. grant (PRAXIS XXI/BD/5117/95).

References

Adams T. F., 1977, ApJS 33,19
Arkhipova V. P., Afanasev V. L., Dostal V. A. et al., 1981, Soviet AJ 25, 277
Baldwin J. A., 1975, ApJ 201, 26
Baldwin J. A., Phillips M. M., Terlevich R., 1981, PASP 93, 5
Balick B., Heckman T. M., 1979, AJ 84, 302
Balzano V. A., 1983, ApJ 268, 602
Binette L., Robinson A., Courvoisier T. J.-L., 1988, A&A 194, 65
Binette L., Wang J., Villar-Martin M., Martin P., Magris G., 1994, ApJ 414, 535
Bonatto C. J., Pastoriza M. G., 1990, ApJ 353, 445
Brotherton M. S., 1996, ApJS 102, 1
Brungardt C. L., 1988, ApJ 327, L51
Cid Fernandez R., Dottori H. A., Gruenwald R. B., Viegas S. M., 1992, MNRAS 255, 165
Clarke M. E., Bolton J. G., Shimmins A. J., 1966, AJP 19, 375
Cohen R. D., Osterbrock D. E., 1981, ApJ 243, 81
Cruz-Gonzalez I., Guichard J., Serrano A., Carrasco L., 1991, PASP 103, 888
Dahari O., 1985, ApJS 57, 643
Dahari O., de Robertis M. M., 1988, ApJS 67, 249
Davidson K., Kinman T. D., 1978, ApJ 227, 776
de Grijp M. H. K., Keel W. C., Miley G. K., Goudfrooij P., Lub J., 1992, A&AS 96, 389
Dekker H., D'Odorico S., Arsenault R., 1988, A&AS 189, 353
Denisyuk E. K., Lipovetski V. A., 1983, Astrophysics 20, 290
de Robertis M. M., 1987, ApJ 316, 597
de Robertis M. M., Osterbrock D. E., 1986, ApJ 301, 727
de Vaucouleurs G., de Vaucouleurs A., Nieto J.-L., 1979, AJ 84, 1811
de Vaucouleurs G., de Vaucouleurs A., Corwin Jr. H. G. et al., 1991, Third reference catalogue of bright galaxies, Springer-Verlag, New-York
Evans I. N., Dopita M. A., 1985, ApJS 58, 125
Fanaroff B. L., Riley J. M., 1974, MNRAS 167, 31P
Feldman F. R., Weedman D. W., Balzano V. A., Ramsey L. W., 1982, ApJ 256, 427
Filippenko A. V., 1985, ApJ 289, 475
Filippenko A. V., 1993, The nearest active galaxies. In: Beckman J. et al. (eds.). CSIC, Madrid, p. 99
Filippenko A. V., Halpern J. P., 1984, ApJ 285, 458
Filippenko A. V., Sargent W. L. W., 1985, ApJS 57, 503
Filippenko A. V., Terlevich R., 1992, ApJ 397, L79
Fiore F., Elvis M., Siemiginowska A. et al., 1995, ApJ 449, 74
Fomalont E. B., 1971, AJ 76, 513
Fruscione A., Griffiths R. E., 1991, ApJ 380, L13
Gaskell C. M., Ferland G. J., 1984, PASP 96, 393
Goodrich R. W., 1989, ApJ 342, 224
Halpern J. P., Oke J. B., 1987, ApJ 312, 91
Halpern J. P., Steiner J. E., 1983, ApJ 269, L37
Heckman T. M., 1980, A&A 87, 152
Heckman T. M., Miley G. K., van Breugel W. J. M., Butcher H. R. 1981, ApJ 247, 403
Heckman T. M., van Breugel W., Miley G. K., Butcher H. R., 1983, AJ 88, 1077
Hill G. J., Healsey J. N., Becklin E. E., Wynn-Williams C. G., 1988, AJ 95, 1031
Ho L. C., Filippenko A. V., Sargent W. L. W., 1993a, ApJ 417, 63
Ho L. C., Shields J. C., Filippenko A. V., 1993b, ApJ 410, 567
Ho L. C., Filippenko A. V., Sargent W. L. W., 1995, ApJS 98, 477
Huchra J. P., 1977, ApJS 35, 171
Huchra J. P., Wyatt W. F., Davis M., 1982, AJ 87, 1628
Hutchings J. B., Neff S. G., 1991, AJ 101, 434
Jackson N., Eracleous M., 1995, MNRAS 276, 1409
Jenkins C. R., 1984, ApJ 277, 501
Keel W. C., 1983a, ApJ 269, 466
Keel W. C., 1983b, ApJS 52, 229
Keel W. C., 1984, ApJ 282, 75

Keel W. C., Kennicutt Jr. R. C., Hummel E., van der Hulst J. M., 1985, AJ 90, 708
Kennicutt R. C., Keel W. C., Blaha C. A., 1989, AJ 97, 1022
Kent S. M., Sargent W. L. W., 1979, ApJ 230, 667
Khachikian E. Y., Weedman D. W., 1974, ApJ 192, 581
Kim D.-C., Sanders D. B., Veilleux S., Mazzarella J. M., Soifer B. T., 1995, ApJS 98, 129
Kingdom J., Ferland G. J., Feibelman W. A., 1995, ApJ 439, 793
Kinney A. L., Bregman J. L., Huggins P. J., Glassgold A. E., Cohen R. D., 1984, PASP 96, 398
Kinney A. L., Antonucci R. R. J., Ward M. J., Wilson A. S., Whittle M., 1991, ApJ 377, 100
Klaas U., Elsasser H., 1991, A&AS 90, 33
Koratkar A., Deustua S. E., Heckman T. et al., 1995, ApJ 440, 132
Koski A. T., 1978, ApJ 223, 56
Kunth D., Sargent W. L. W., 1979, A&A 76, 50
Laor A., Netzer H., 1989, MNRAS 238, 897
Leahy J. P., Perley R. A., 1991, AJ 102, 537
Lemaîitre G., Kohler D., Lacroix D., Meunier J.-P., Vin A., 1989, A&A 228, 546
Lequeux J., Peimbert M., Rayo J. F., Serrano A., Torres-Peimbert S., 1979, A&A 80, 155
Lonsdale C. J., Lonsdale C. J., Smith H. E., 1992, ApJ 391, 629
MacAlpine G. M., Davidson K., Gull T. R., Wu C.-C., 1985, ApJ 294, 147
MacKenty J. W., 1990, ApJS 72, 231
Malkan M. A., 1983, ApJ 264, L1
Maltby P., Matthews T. A., Moffet A. T., 1962, ApJ 137, 153
Maoz D., Filippenko A. V., Ho L. C. et al., 1995, ApJ 490, 91
Mazzarella J. M., Boroson T. A., 1993, ApJS 85, 27
McCall N. L., Rybski P. M., Shields G. A., 1985, ApJS 57,1
McQuade K., Calzetti D., Kinney A. L., 1995, ApJS 97, 331
Moorwood A. F. M., van der Werf P. P., Kotilainen J. K., Marconi A., Oliva E., 1996, A&A 308, L1
Nelson C. H., MacKenty J. W., Simkin S. M., Griffiths R. E., 1996, ApJ (in press)
Netzer H., Laor A., 1993, ApJ 404, L51
Osmer P. S., Smith M. G., Weedman D. W., 1974, ApJ 192, 279
Oke J. B., 1990, AJ 99, 1621
Oke J. B., Gunn J. E., 1983, ApJ 266, 713
Osterbrock D. E., 1974, Astrophysics of gaseous nebulae. Freeman and company, San Francisco
Osterbrock D. E., 1977, ApJ 215, 733
Osterbrock D. E., 1981, ApJ 249, 452
Osterbrock D. E., 1985, PASP 97, 25
Osterbrock D. E., Dahari O., 1983, ApJ 273, 478
Osterbrock D. E., de Robertis M. M., 1985, PASP 97, 1129
Osterbrock D. E., Pogge R. W., 1985, ApJ 297, 166
Osterbrock D. E., Tran H. D., Veilleux S., 1992, ApJ 389, 196
Owen F. N., Laing R. A., 1989, MNRAS 238, 357
Owen F. N., Ledlow M. J., Keel W. C., 1996, AJ 111, 53
Phillips M. M., Charles P. A., Baldwin J. A., 1983, ApJ 266, 485
Popov V. N., Khachikian E. E., 1980, Astrophysics 16, 33
Riley J. M., Pooley G. G., 1975, Mem. RAS 80, 105
Robinson A., Binette L., Fosbury R. A. E., Tadhunter C. N., 1987, MNRAS 227, 97
Rosenblatt E. J., Malkan M. A., Sargent W. L. W., Readhead A. C. S., 1994, ApJS 93, 73
Sakka K., Oka S., Wakamatsu K., 1973, PASJ 25, 153
Sandage A., Tammann G. A., 1981, A revised Shapley-Ames catalog of bright galaxies. In: Carnegie Institution of Washington, Publication 635
Schmidt M., 1965, ApJ 141, 1
Schulz H., Fritsch C., 1994, A&A 291, 713
Sersic J.-L., Pastoriza M., 1965, PASP 77, 287
Seyfert K., 1943, ApJ 97, 28
Shields J. C., 1992, ApJ 399, L27
Shields J. C., Filippenko A. V., 1990, AJ 100, 1034
Shuder J. M., Osterbrock D. E., 1981, ApJ 250, 55
Simkin S. M., 1979, ApJ 234, 56
Smith E. P., Heckman T. M., 1989, ApJS 69, 365
Stasinska G., 1984, A&A 135, 341
Stauffer J. R., 1982, ApJ 262, 66
Stockton A. N., 1968, AJ 73, 887
Stone R. P. S., 1977, ApJ 218, 767
Storchi-Bergmann T., 1991, MNRAS 249, 404
Storchi-Bergmann T., Pastoriza M. G., 1989, ApJ 347, 195
Storchi-Bergmann T., Kinney A. L., Challis P., 1995, ApJS 98, 103
Terlevich R., Melnick J., 1985, MNRAS 213, 841
Terlevich R., Melnick J., Masegosa J., Moles M., Copetti M. V. F., 1991, A&AS 91, 285
Tran H. D., 1995, ApJ 440, 578
Tran H. D., Miller J. S., Kay L. E., 1992, ApJ 397, 452
Veilleux S., 1988, AJ 95, 1695
Veilleux S., 1991, ApJ 368, 158
Veilleux S., Osterbrock D. E., 1987, ApJS 63, 295
Véron M.-P., 1981, A&A 100,12
Véron M.-P., Véron P., Zuiderwijk E. J., 1981b, A&A 98, 34
Véron-Cetty M.-P., Véron P., 1985, A&A 145, 425
Véron-Cetty M.-P., Véron P., 1986a, A&AS 65, 241
Véron-Cetty M.-P., Véron P., 1986b, A&AS 66, 335
Véron-Cetty M.-P., Véron P., 1996, A&AS 115, 97
Véron P., Linblad P. O., Zuiderwijk E. J., Véron M.-P., Adam G., 1980, A&A 87, 245
Véron P., Véron-Cetty M.-P., Bergeron J., Zuiderwijk E. J., 1981a, A&A 97, 71
Véron P., Véron-Cetty M.-P., Zuiderwijk E. J., 1981c, A&A 102, 116
Véron P., Véron-Cetty M.-P., 1986, A&A 161, 145
Vorontsov-Velyaminov B. A., 1977, A&AS 28, 1
Vrtilek J. M., Carleton N. P., 1985, ApJ 294, 106
Wagner S. J., 1988, PASP 100, 54
Ward M., Penston M. V., Blades J. C., Turtle A. J., 1980, MNRAS 193, 563
Weedman D. W., Feldman F. R., Balzano V. A. et al., 1981, ApJ 248, 105
Whitford A. E., 1958, AJ 63, 201
Whittle M., 1985a, MNRAS 213, 1
Whittle M., 1985b, MNRAS 213, 33
Wilson A. S., Heckman T. R., 1985, in: Astrophysics of active galaxies and quasistellar objects, ed. Miller J. S., Reidel, Dordrecht, p. 39
Wyndham J. D., 1966, ApJ 144, 459
Yee H. K. C., Oke J. B., 1978, ApJ 226, 753
Young S., Hough J. H., Bailey J. A., Axon D. J., Ward M. J., 1993, MNRAS 260, L1
Zamorano J., Rego M., Gallego J. et al., 1994, ApJS 95, 387

This article was processed by the author using Springer-Verlag LaTeX A&A style file *L-AA* version 3.